Journal of Polyphenols
2024, 6 (3): 117–129
journal homepage: http://jpolyph.syphu.edu.cn

Optimization of extraction process for total flavonoids of Sophorae Flos for the treatment of hyperlipidemia based on network pharmacology and molecular docking

Jiale Mao †, Aijinxiu Ma †, Lingling Wang, Xu Zhao *

Faculty of Functional Food and Wine, Shenyang Pharmaceutical University, Shenyang 110016, China

Abstract This study aimed to investigate the mechanism of action of Sophora Flos (SF) in the treatment of hyperlipidemia (HLP) using network pharmacology and molecular docking methods, and to optimize the extraction process of the predicted active components. The STRING database was used for protein interaction analysis and PPI network construction via Cytoscape 3.9.1. Pymol was employed for docking and visualization. An extensive review of SF identified 6 active ingredients, 297 related objectives, 84 disease objectives, and 57 total objectives. After protein interaction and topology analysis, 18 core targets were identified. These included 146 gene function entries ($P < 0.05$). Active compounds, mainly flavonoids, can modulate the expression of various proteins such as TNF, IL-6, IL-1β, PPARG, and TGFB1 to achieve therapeutic effects on HLP. The network pharmacology and molecular docking results suggested that the active flavonoids component in SF may be related to the treatment of hyperlipidemia. Therefore, the orthogonal experiment method was used to optimize the extraction process of total flavonoid from SF using ethanol reflux extraction, based on a single factor experiment. The effects of reflux time, solid-liquid ratio, ethanol concentration, and other factors on the extraction of total flavonoid from SF were investigated. The optimum process conditions were reflux time of 1.25 h, solid-liquid ratio of 1:15 g/mL and ethanol concentration of 60%. Using these conditions, the purity of total flavonoid extracted from SF was 70.33 ± 0.22%.

Keywords: Sophorae Flos; total flavonoid; process optimization; network pharmacology; hyperlipidemia

1 Introduction

Hyperlipidemia (HLP) is a medical condition where the blood lipid levels exceed the normal range due to abnormal fat metabolism [1]. Sophorae Flos (SF) is the dried flower buds of *Sophora japonica* L., which has the functions of cooling blood, hemostasis and clearing liver. SF has been used in traditional Chinese medicine for a long time [2]. Modern medical research has shown that SF contains various active substances such as flavonoids, polysaccharides, essential oils, polyphenols, and others [3]. Network pharmacology is a TCM, including multi-component, multi-target, and synergy research approach that uses systems biology, pharmacology, and computational analysis to unravel the mechanism of drug action, adopting a multi-component network and target action research mode, which is consistent with the characteristics of action [4]. The study used network pharmacology and molecular docking technology to establish a database of relevant targets of SF for the treatment of hyperlipidemia,

* Corresponding author: Xu Zhao (zhaoxu_1010@163.com).
† These authors contributed equally to this work;
These authors have no conflict of interest to declare.

established the network relationship between target genes and pathways, and investigated the key pathways, to provide a reference for elucidating the mechanism of action of SF for the treatment of hyperlipidemia.

Several studies have shown that flavonoids are effective in improving hyperlipidemia [5, 6]. SF contains several flavonoids active constituents, including rutin, nicotiflorin, narcissoside, kaempferol, isorhamnetin, quercetin, and total flavonoid of SF [7]. Rutin has been shown to prevent hyperlipidemia-induced lipotoxicity and immune activation in rats [8]. Currently, the most widely used extraction method is the ethanol reflux method, but this method is expensive due to the large number of organic solvents required, making it unsuitable for industrial production. The aim of this study was to optimize the extraction process of SF flavonoids by means of an orthogonal experiment based on single factor experiment, and the best extraction process was determined using the total flavonoid content as index.

2 Materials and methods

2.1 Materials and reagents

SF powder was purchased from Shanghai Jinliang Food Technology Co., Ltd (Shanghai, China), and rutin control was purchased from Dalian Meilun Biotechnology Co., Ltd (Dalian, China). Distilled water was purchased from Hangzhou Wahaha Beverages Co (Hangzhou, China). Anhydrous ethanol was purchased from Tianjin Li'anlong Bohua Pharmaceutical Chemistry Co. Ltd (Tianjin, China). NaOH was purchased from Tianjin Ruijinte Chemicals Co. Ltd (Tianjin, China). Anhydrous $AlCl_3$ was purchased from Fuchen Chemical Reagent Co (Tianjin, China). $NaNO_2$ was purchased from Tianjin Hengxing Chemical Reagent Manufacturing Co (Tianjin, China).

2.2 Network pharmacology

2.2.1 Collection of active ingredients of SF

The Traditional Chinese Medicine Systematic Pharmacology Database and Analysis Platform (TCMSP, https://www.tcmsp-e.com/) was used to identify the active ingredients of SF. For the study, only those active ingredients with oral bioavailability (OB) ≥ 30% and drug-likeness (DL) ≥ 0.18 were selected. The corresponding target for each active ingredient was retrieved from the TCMSP database, and the UniProt ID of the corresponding target was obtained from the UniProt database (https://www.uniprot.org/). The gene name was acquired from the UniProt database via the Gene symbol.

2.2.2 Collection of potential targets of SF and HLP

Targets related to hyperlipidemia (HLP) were identified by searching GeneCards, OMIM, and TTD databases using the keyword "hyperlipidemia". The HLP-associated targets were merged with those in the GeneCards database with a relevance score of 1 or higher. After removing duplicates, the HLP-associated targets were obtained. Venny2.1.0 was used to generate Wayne diagrams of potential SF agent and HLP targets, and common SF agent and HLP targets were obtained by intersection.

2.2.3 Construction of protein-protein interaction network

The STRING database was used to generate a protein-protein interaction network diagram identifying potential targets for SF treatment of HLP. To search for multiple proteins, simply enter the protein name in the search box, select "Homo sapiens" as the species, and select high confidence. The other parameters are system defaults. Once the network diagram has been generated, the TSV file can be downloaded and imported into Cytoscape 3.9.1 for further visualization and analysis. To perform the topological analysis, Cytoscape Network Analysis plug-in was used, which used median degree, closeness, and betweenness as thresholds to exclude the key targets of the SF from HLP treatment and build the protein-protein interaction networks of the core targets.

2.2.4 GO and KEGG function enrichment analysis

The identified targets were uploaded to the DAVID database (https://david.ncifcrf.gov/) for gene ontology (GO) functional annotation and Kyoto Encyclopedia of Genes and Genomes (KEGG, https://www.kegg.jp/) pathway enrichment analysis. Sapiens. The condition filter used was $P < 0.05$. For visual analysis, the top 10 entries were selected for each biological process (BP), cellular component (CC), and molecular function (MF) in the GO functional annotation, as well as the top 20 pathways in the KEGG pathway enrichment.

2.2.5 Molecular docking simulation

The three most prominent targets, chosen based on their degree values in the PPI network, underwent molecular docking with their corresponding key components. The components and target protein structures were obtained from the Protein Data Bank (PDB) and PubChem database (https://pubchem.ncbi.nlm.nih.gov/), respectively. The process of molecular docking was carried out using AutoDockTools, and the visualization was done using Pymol. Combined with previous literature reports, the docking model with the lowest binding energy was selected.

2.3 Optimization of the extraction process

2.3.1 Preparation of standard solutions

40 mg of rutin standard was accurately weighed, a small amount of 60% ethanol solution was added, the solution was dissolved by heating in a water bath and the solution was transferred to a 100 mL volumetric flask. The above steps were repeated until all the rutin standards was transferred to the volumetric flask. The rutin standard solution with a concentration of 400 mg/L was obtained.

2.3.2 Samples handling

4.0 mL of 60% sample solution and 0.3 mL of 5% $NaNO_2$ solution were added to 1.0 mL of rutin standard solution in a beaker. The mixture was allowed to stand for 8 minutes before 0.3 mL of 10% $AlCl_3$ solution was added, followed by 4.0 mL of 4% NaOH solution, and the resulting solution was transferred to a 10 mL volumetric flask. The solution was diluted to the scale with 60% ethanol solution, shaken well and left to stand for 10 min.

2.3.3 Plotting of standard curves

20 mg rutin standard was accurately weighed, a small amount of 60% ethanol solution was added, the solution was dissolved by water bath heating, and the solution was transferred to a 100 mL volumetric flask. The above steps were repeated until all the rutin standards was transferred to the volumetric flask. The rutin standard solution with a concentration of 200 mg/L was obtained.

0.0, 0.5, 1.0, 1.5, 2.0, 2.5, 3.0 mL of 200 mg/L rutin standard solution were accurately extracted and placed in 10 mL test tubes, respectively. The standard series of 0, 10, 20, 30, 40, 50, 60 μg/mL were prepared according to the method of 2.3.2, and the absorbance values were determined. The standard curve of rutin was obtained by taking the concentration gradient of rutin as abscissa and the absorbance as ordinate. The regression equation was $y = 0.011\ 1x + 0.13 \times 10^{-2}$, and the correlation coefficient was $r = 0.999\ 3$.

2.3.4 Single factor experiment

The SF crude powder was precisely weighed and extracted using a water bath heating reflux with an ethanol solution. A single factor test was conducted on several factors that significantly affect the total flavonoid content, including solid-liquid ratio, extraction time, ethanol concentration, and reflux times, to determine the optimal extraction conditions.

The solid-liquid ratio tests were 1:5, 1:10, 1:15, 1:20 and 1:25 g/mL. The extraction process was run for different times of 0.5, 1, 1.5, 2 and 2.5 h. The number of reflux times was varied, with the options of 1, 2 or 3 times, and the ethanol concentration was varied from 0%, 40%, 60%, 80% and 100%.

2.3.5 Orthogonal test

According to the results of single factor experiment, L_9 (3^4) orthogonal test was used to optimize the extraction conditions of reflux time (A), solid-liquid ratio (B) and ethanol concentration (C), as shown in Table 1.

Table 1 Factor level of SF orthogonal test

Level	A Reflux time (h)	B Solid-liquid ratio (g/mL)	C Ethanol concentration (%)
1	1.25	1:12	50
2	1.5	1:15	60
3	1.75	1:18	70

2.3.6 Determination of samples

A 0.2 mL sample solution was placed in a 10 mL volumetric flask and prepared into a test solution using the method outlined in 2.3.2. The blank solution, without NaOH reagent, was used for comparison, and the absorbance value was recorded. The concentration of total flavonoid in the sample was then calculated using the standard curve.

2.3.7 Determination of Total Flavonoid Purity

The microporous resin of type D101, AB-8, and HPD400 was dissolved by immersion in anhydrous ethanol for 24 h. It was then repeatedly rinsed with distilled water until it was free of any alcoholic taste and set aside. The crude extract of SF total flavonoid was then poured into the pretreated microporous resin and eluted with 30%, 60%, and 90% concentrations of ethanol, and the total flavonoid purity was calculated after combining the concentrated eluates.

Total flavonoid purity = (total flavonoid post-elution/total flavonoid pre-elution) × 100%.

3 Results

3.1 Network pharmacological results

3.1.1 The chemical components of SF

According to the data presented in Table 2, it was found that 6 active substances of SF were identified through the screening of major compounds from the TCMSP database with the conditions OB ≥ 30% and DL ≥ 0.18.

Table 2 Active ingredients of SF

MOL ID	Molecule	OB (%)	DL
MOL000354	Isorhamnetin	49.60	0.31
MOL000358	Beta-sitosterol	36.91	0.75
MOL000422	Kaempferol	41.88	0.24
MOL005935	N-[6-(9-acridinylamino)hexyl]benzamide	41.70	0.78
MOL005940	Quercetin-3'-methyl ether	46.44	0.30
MOL000098	Quercetin	46.43	0.28

3.1.2 Construction of PPI network

The drug targets were predicted based on the TCMSP database, and 178 drug targets were obtained after finding the abbreviations and de-duplicating in the UniProt database. In addition, 584 HLP-related targets were identified from GeneCards, OMIM, and TTD databases after removing duplicates. Venny 2.1.0 software was used to perform Wayne diagram analysis on the drug targets for SF and the HLP disease targets obtained above, resulting in a total of 57 action targets (Fig. 1). The drug-target network was constructed

using Cytoscape software and the results were shown in Fig. 2. Following topological analysis of the protein-protein interaction network obtained from the STRING platform using the Cytoscape software plug-in Network Analysis, 18 core nodes were identified in Fig. 3.

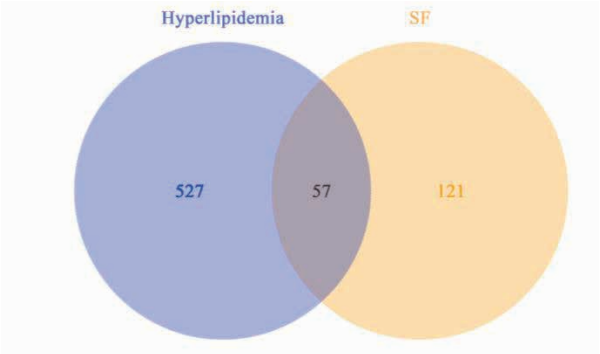

Fig. 1 Venn diagram

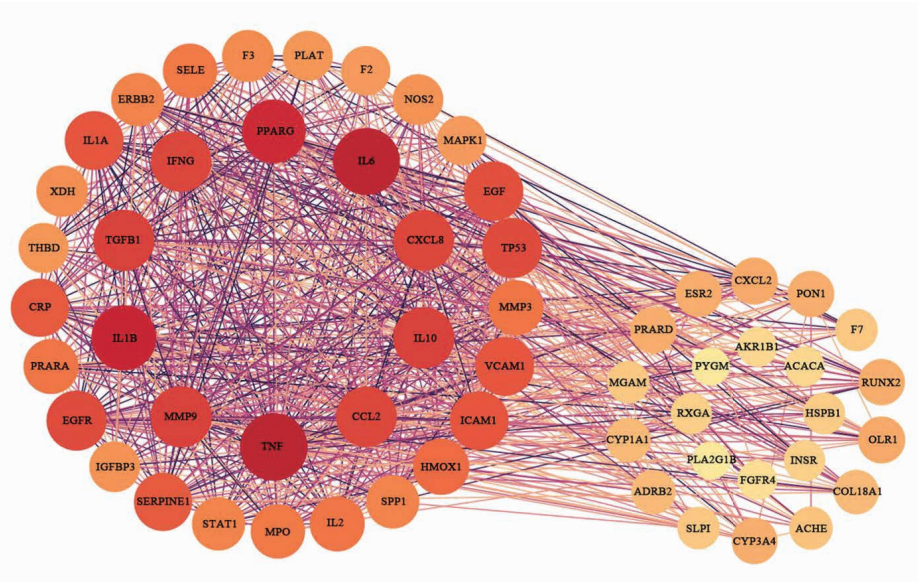

Fig. 2 The "SF-HLP common target" network

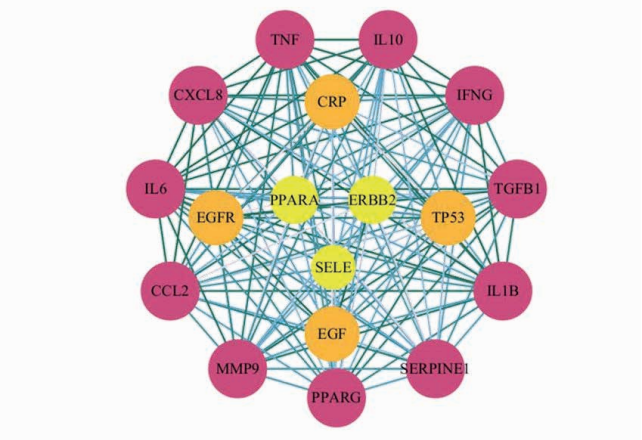

Fig. 3 The "screened key SF-HLP common target" network

3.1.3 GO and KEGG enrichment analysis

Functional annotation of key targets was performed using DAVID and the results were shown in Fig. 4. 225 of the annotations were found to be related to BP, including positive regulation of gene expression and cellular response to lipopolysaccharide. In addition, 3 annotations were related to positive regulation of pri-miRNA transcription from RNA polymerase II promoter. Furthermore, 11 annotations were annotated to be related to CC. There are 11 annotations related to CC, such as extracellular space, extracellular region, and platelet alpha granule lumen. In addition, there were 22 annotations related to MF, including cytokine activity, protein phosphatase activity, and growth factor activity. It is worth noting that there were 22 MF-related annotations, including cytokine activity, protein phosphatase binding, and growth factor activity.

According to Fig. 5, the results of the pathway enrichment analysis of key targets by DAVID indicated that eighty-nine signaling pathways were enriched for the key targets of SF for HLP treatment. Among the main pathways that were enriched, the result showed malaria, Chagas disease, the AGE-RAGE signaling pathway in diabetic complications, lipid and atherosclerosis, and African trypanosomiasis.

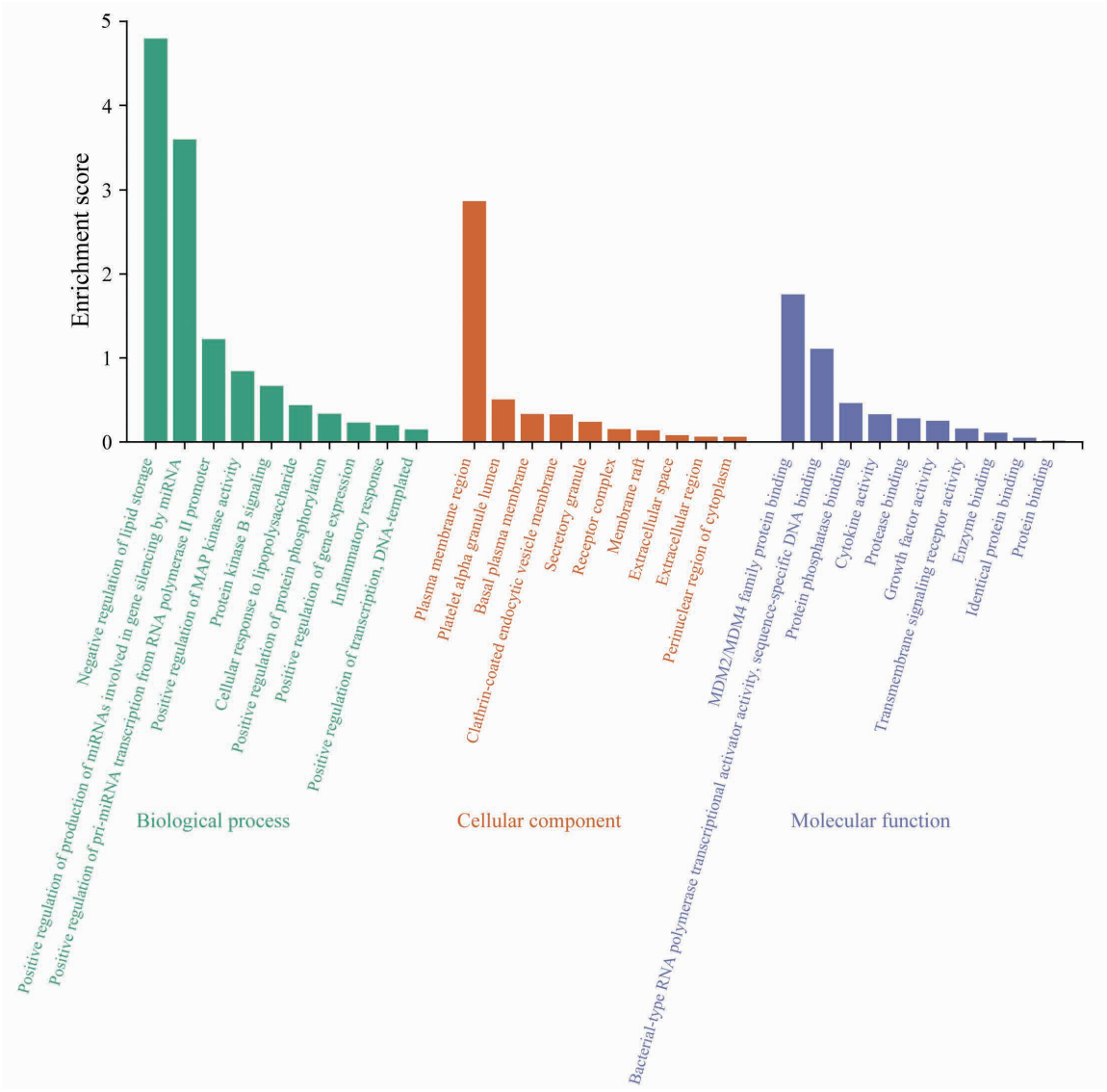

Fig. 4 GO function enrichment analysis

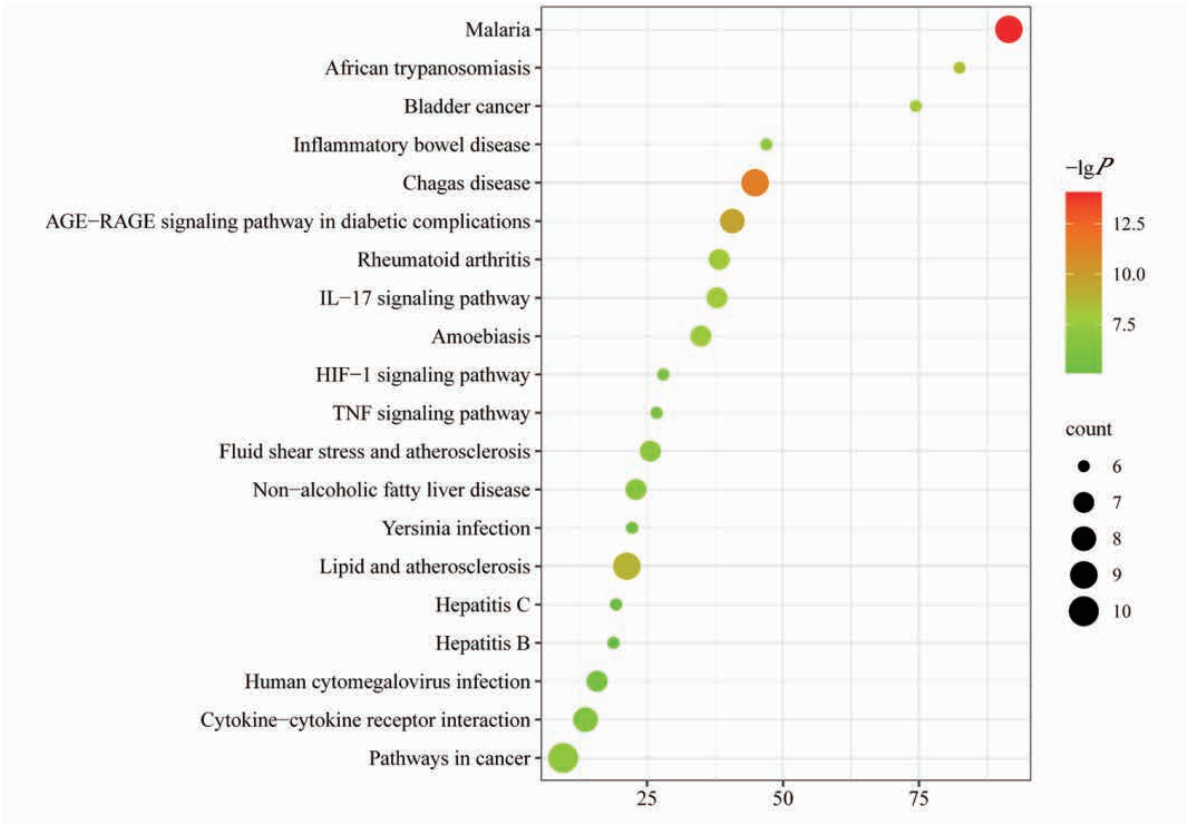

Fig. 5 KEGG function enrichment analysis

3.1.4 Docking results of SF key components with key target proteins

Among the 18 key common targets, the top three targets TNF, IL-6, IL-1β and their corresponding two flavonoid active ingredients quercetin and kaempferol were screened for molecular docking according to Degree. The molecular docking results suggested that the flavonoids component quercetin and kaempferol in SF had strong binding activity with the core targets IL-1β, IL-6, and TNF, with binding energies less than −5 kcal/mol (1 cal = 4.4 J)，as shown in Table 3. These two active components were believed to be important in the treatment of HLP with SF. The docking results were visualized using Pymol software, as shown in Fig. 6.

Table 3 Molecular docking results between representative SF active ingredients and the signaling pathway targets

Target name	PDB ID	Compound	Mol ID	Binding energy
IL-1β	31BI	Quercetin	MOL000098	−13.9
TNF	2ZJC	Quercetin	MOL000098	−8.9
IL-6	1IL6	Quercetin	MOL000098	−5.9
IL-6	1IL6	Kaempferol	MOL000422	−5.8

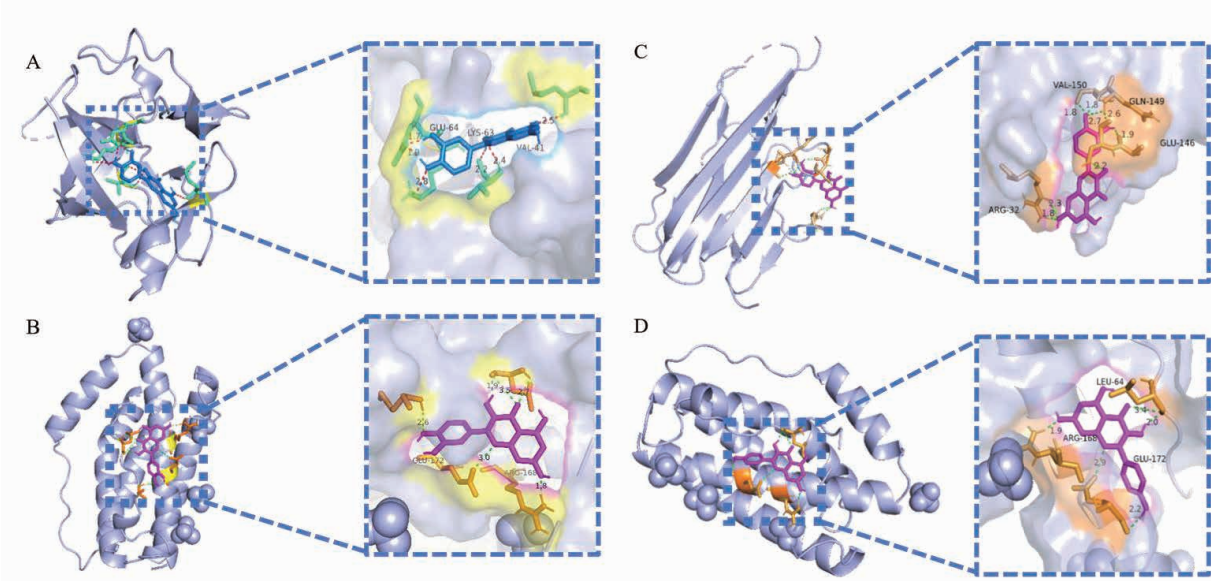

A − IL-1*β*-quercetin; B − IL-6-quercetin; C − TNF-quercetin; D − IL-6-kaempferol.

Fig. 6 Molecular docking simulation of bioactive compound-key target

3.3 Process optimization results

3.3.1 Results of single factor test

The SF powder was refluxed in a 60% ethanol solution for one, two, and three cycles at a ratio of 1:15 g/mL for 1.5 h. As shown in Fig. 7 (A), the results of the test indicated that the time of reflux cycles did not have a significant effect on the total flavonoid content. Thus, to reduce costs, it was decided to reflux the powder only once for the subsequent tests. The reflux time was set at 0.5, 1, 1.5, 2 and 2.5 h with a solid-liquid ratio of 1:15 g/mL and an extraction temperature of 85 ℃. The optimal extraction time was found to be 1.5 hours from Fig. 7 (B). Fig. 7 (C) showed optimal extraction time for solid-liquid ratio ($M_{SF\ mass}/V_{water\ volume}$) of 60% at 1:5, 1:10, 1:15, 1:20 and 1:25 g/mL. The effect of solid-liquid ratio on total flavonoid content after 1.5 hours of reflux extraction in ethanol solution at 85 °C in a water bath was investigated. The results showed That the highest content was observed when the solid-liquid ratio was 1:15 g/mL. Fig. 7 (D) showed the total flavonoid results after fixed reflux time of 1.5 h, solid-liquid ratio of 1:15 g/mL, water bath temperature of 85 °C and reflux extraction at 0%, 40%, 60%, 80%, and 100% ethanol concentration. The study suggested that the total flavonoid content of SF initially increased and then decreased with increasing ethanol concentration. This phenomenon could be attributed to cell wall calcification caused by high ethanol concentration, resulting in a decrease in the total flavonoid extraction rate. The highest total flavonoid content was observed at 60% ethanol concentration. Therefore, after careful consideration, it was determined that the most optimal extraction conditions for SF would be 1 reflux cycle, 1.5 hours reflux time, solid-liquid ratio of 1:15 g/mL, and 60% ethanol concentration, and these conditions were selected for subsequent experiments.

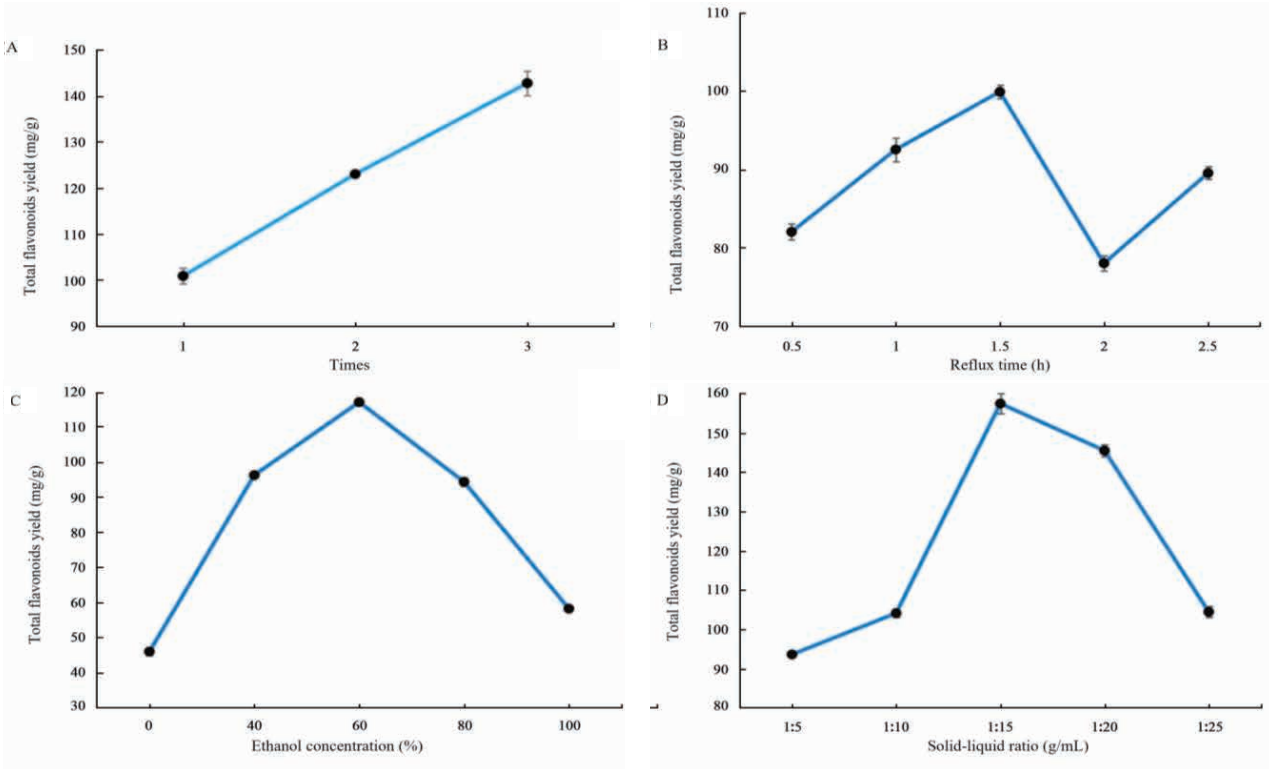

(A) − Times; (B) − Reflux time; (C) − Ethanol concentration; (D) − Solid-liquid ratio

Fig. 7 Effect of four factors on the yield of total flavonoid extraction from SF

3.3.2 Result of orthogonal experimental

The total flavonoid content of each experimental group was determined using orthogonal design, experimental data were visually analyzed and analysis of variance (ANOVA), results were presented in Table 4 and Table 5. ANOVA indicated that. neither ethanol concentration (C) nor reflux time (A) had a significant effect on total flavonoid content ($P > 0.05$). Notably, the solid-liquid ratio had a significant influence ($P < 0.05$). The extraction method with the highest total flavonoid content was $A_1B_2C_2$, with 1.25 h reflux time, 1:15 g/mL solid-liquid ratio, and 60% ethanol concentration.

Table 4 Orthogonal test results of total flavonoid extraction from SF

Level	A	B	C	Total flavonoid yield (mg/g)
1	1	1	1	96.82
2	1	2	2	135.2
3	1	3	3	85.56
4	2	1	2	93.73
5	2	2	3	83.42
6	2	3	1	110.8
7	3	1	3	93.73
8	3	2	1	85.35
9	3	3	2	104.8

(to be continued)

Continued Table 4

Level	A	B	C	Total flavonoid yield (mg/g)
K_1	317.59	284.28	292.93	
K_2	287.90	303.98	333.78	
K_3	283.90	301.14	262.70	
R	11.23	6.57	23.69	
Optimal level	A_1	B_2	C_2	
Factor effects		C > A > B		
Optimal combinations		$A_1 B_2 C_2$		

Table 5 ANOVA of Orthogonal test results

Factor	SS	df	MS	*F*	*P*	Significant
A	225.86	2	112.93	0.22	0.06	
B	75.60	2	37.80	0.08	0.02	*
C	847.96	2	423.98	0.84	0.21	

Note: SS: Sum of the square; df: Degree of freedom; MS: Mean of the square; F: F-value; *: $P < 0.05$; A: Reflux time; B: Solid-liquid ratio; C: Ethanol concentration.

3.3.3 Total flavonoid purification results

Optimization of the extraction and purification process of total flavonoid from SF using different types of microporous adsorbent resins resulted in purified SF extracts of 65.48 ± 0.02% purity for AB-8, 62.02 ± 0.29% for HPD400 and 70.33 ± 0.22% for D101.

4 Discussion

The high prevalence of HLP has been identified as an independent risk factor for cardiovascular, and cerebrovascular disease [9-11]. This process includes lipid accumulation, plaque progression, and thrombosis, with inflammation playing an important part. Notably, inflammatory mediators are significantly increased in patients with peripheral arterial disease (PAD) [12, 13]. Such an imbalance may result in the accumulation of excess fatty substances in the vascular endothelium, accelerating the atherogenic process and increasing the risk of stroke [14-16].

The study used network pharmacology, molecular docking, and molecular biology to explore the active components of SF and their potential mechanism of action in the treatment of PAD. Based on OB and DL screening, seven potential active ingredients were identified from TCMSP. They also act as natural antioxidants to counter free radical oxidation, stop free radical chain reactions, inhibit peroxidation of unsaturated fatty acids on biofilm, and scavenge lipid peroxidation products, thus helping to protect the integrity of biological membranes and subcellular structures, playing an important role *in vivo* [17-19]. Rutin has shown to reduce the level of malondialdehyde (MDA) and increase the activity of superoxide dismutase (SOD) in tissue, which can improve the immune and antioxidant capacity of the body, reduce free radical damage and have a significant protective effect on a series of inflammatory cascades generated by dysregulated lipid metabolism *in vivo* [20-23].

According to the PPI network analysis, TNF, IL-6, and IL-1β were found to be the key targets of SF for the treatment of HLP. It worthed noting that prolonged HLP could potentially impair

vascular endothelial function, activate inflammatory mediators, and induce an inflammatory response. At the same time, the overproduction of inflammatory mediators could trigger an inflammatory cascading reaction that accelerates vascular lipid accumulation and endothelial damaged. In a persistent state of hyperlipidemia, it was important to not only treat but also indirectly reduce the inflammatory response. It should be noted that TNF-α is mainly produced by T lymphocytes and its biological role is to trigger inflammatory responses and antitumor activity. As a pro-inflammatory mediator, TNF-α can induce other inflammatory mediators, such as IL-6, thereby promoting the development of atherosclerosis. In addition, TNF-α serves as a reflective indicator of the early stage of inflammation [24-26].

Analysis of overlapping targets by GO and KEGG pathway enrichment suggested that SF exerts its therapeutic effect on HLP primarily by targeting malaria, lipid and atherosclerosis, and AGE-RAGE pathways. This may be due to the ability of key components in SF to inhibit the inflammatory response, which is present throughout the HLP process and serves as an initiator of atherosclerosis. It has been observed that IL-6, which is produced by various immune cells such as T lymphocytes, B lymphocytes, and macrophages, plays a role in response to infection *in vivo* [27, 28]. IL-6 also promotes vascular inflammation through increased macrophage uptake of LDL-C, accelerated lipid accumulation, vascular smooth muscle cell proliferation, and increased expression of adhesion molecules and other cytokines [29-31]. The research suggested that SF components may have the ability to inhibit IL-6 expression, reduce inflammatory mediators, and inhibit the onset and development of HLP. Additionally, the molecular docking results indicated that quercetin and kaempferol had strong binding activities with the three target proteins, TNF, IL-6, and IL-1β, and formed stable conformations through intermolecular forces such as hydrogen bonding.

Various methods have been used to extract total flavonoid from SF, including alkaline acid precipitation, hot alcohol extraction, ultrasonic extraction, and microwave extraction [32-34]. However, these methods have some shortcomings, such as low extraction efficiency, long process time, high cost, low purity of extracted rutin, and high incandescent residue. To obtain the total flavonoid active ingredients cost-effectively and efficiently, this study used the ethanol reflux extraction method to improve the traditional process.

5 Conclusion

Through network pharmacology and molecular docking, the results suggested that flavonoids in SF had the potential to modulate pathways including TNF, IL-6, and IL-1β, thereby inhibiting the occurrence of inflammatory reactions and that SF could be a multi-component, multi-target, multi-method treatment for HLP. The optimal extraction process for total flavonoid in SF was determined by single factor and orthogonal tests. The total flavonoid purity of the extract reached 70.33 ± 0.22% with good reproducibility and stability, confirming the rationality and feasibility of the process. Further *in vitro* and *in vivo* studies are needed to validate the results.

References

[1] Yao YS, Li TD, Zeng ZH. Mechanisms underlying direct actions of hyperlipidemia on myocardium: An updated review [J]. Lipids Health Dis, 2020, 19 (1): 23.

[2] Chen Y, Chen LM, Tong Y, et al. Pharmacological effect and toxicology of Sophorae Tonkinensis Radix et Rhizoma [J]. China Journal of Chinese Materia Medica, 2017, 42 (13): 2439-2442.

[3] Li R, Wang C, Lei P, et al. Chemical constituents in Flos Sophorae Carbonisatus [J]. China Journal of Chinese Materia Medica, 2010, 35 (5): 607-609.

[4] Zhao L, Zhang H, Li N, et al. Network pharmacology, a promising approach to reveal the pharmacology mechanism of Chinese medicine formula [J]. J Ethnopharmacol, 2023, 309: 116306.

[5] Li Y, Chen X, Xue J, et al. Flavonoids furom Coreopsis tinctoria adjust lipid metabolism in hyperlipidemia animals by down-regulating adipose differentiation-related

protein [J]. Lipids Health Dis, 2014, 13: 193.

[6] Bai YF, Yue ZL, Wang YN, et al. Synergistic effect of polysaccharides and flavonoids on lipid and gut microbiota in hyperlipidemic rats [J]. Food Funct, 2023, 14 (2): 921-933.

[7] Fan S, Yang G, Zhang J, et al. Optimization of ultrasound-assisted extraction using response surface methodology for simultaneous quantitation of six flavonoids in Flos Sophorae Immaturus and antioxidant activity [J]. Molecules, 2020, 25 (8): 1767.

[8] Manzoni AG, Passos DF, Leitemperger JW, et al. Hyperlipidemia-induced lipotoxicity and immune activation in rats are prevented by curcumin and rutin [J]. Int Immunopharmacol, 2020, 81: 106217.

[9] Li Z, Zhu G, Chen G, et al. Distribution of lipid levels and prevalence of hyperlipidemia: Data from the NHANES 2007-2018 [J]. Lipids Health Dis, 2022, 21 (1): 111.

[10] Alloubani A, Nimer R, Samara R. Relationship between hyperlipidemia, cardiovascular disease and stroke: A systematic review [J]. Curr Cardiol Rev, 2021, 17 (6): e051121189015.

[11] Xiang Y, Mao L, Zuo ML, et al. The role of microRNAs in hyperlipidemia: From pathogenesis to therapeutical application [J]. Mediators Inflamm, 2022, 2022: 3101900.

[12] Yang ST, Liu CH, Wang PH. The impact of hyperlipidemia and carotid atherosclerosis [J]. J Chin Med Assoc, 2023, 86 (4): 451-452.

[13] Suh JS, Kim SYJ, Lee SH, et al. Hyperlipidemia is necessary for the initiation and progression of atherosclerosis by severe periodontitis in mice [J]. Mol Med Rep, 2022, 26 (2): 273.

[14] Wang C, Du Z, Ye N, et al. Hyperlipidemia and hypertension have synergistic interaction on ischemic stroke: Insights from a general population survey in China [J]. BMC Cardiovasc Disord, 2022, 22 (1): 47.

[15] Lu S, Yuan Y, Chen F, et al. Holothuria leucospilota polysaccharides alleviate hyperlipidemia via alteration of lipid metabolism and inflammation-related gene expression [J]. J Food Biochem, 2022, 46 (12): e14392.

[16] Zhao H, Li Y. Upregulated microRNA-185-3p inhibits the development of hyperlipidemia in rats [J]. Kidney Blood Press Res, 2023, 48 (1): 35-44.

[17] Chen J, Wu J, Mu J, et al. An antioxidative sophora exosome-encapsulated hydrogel promotes spinal cord repair by regulating oxidative stress microenvironment [J]. Nanomedicine, 2023, 47: 102625.

[18] Wang F, Zhao X, Su X, et al. Isorhamnetin, the xanthine oxidase inhibitor from Sophora japonica, ameliorates uric acid levels and renal function in hyperuricemic mice [J]. Food Funct, 2021, 12 (24): 12503-12512.

[19] Liu Y, Huang W, Ji S, et al. Sophora japonica flowers and their main phytochemical, rutin, regulate chemically induced murine colitis in association with targeting the NF-kappaB signaling pathway and gut microbiota [J]. Food Chem, 2022, 393: 133395.

[20] Sun C, Wang L, Sun J, et al. Hypoglycemic and hypolipidemic effects of rutin on hyperglycemic rats [J]. J Tradit Chin Med, 2020, 40 (4): 640-645.

[21] Zhou J, Liu Q, Yang Z, et al. Rutin maintains redox balance to relieve oxidative stress induced by TBHP in nucleus pulposus cells [J]. In Vitro Cell Dev Biol Anim, 2021, 57 (4): 448-456.

[22] Bermejo-Bescos P, Jimenez-Aliaga KL, Benedi J, et al. A diet containing rutin ameliorates brain intracellular redox homeostasis in a mouse model of Alzheimer's disease [J]. Int J Mol Sci, 2023, 24 (5): 4863.

[23] Liang XH, Han YY, Wang S, et al. Anti-aging effect of rutin in caenorhabditis elegans and D-Gal-induced aging mouse model [J]. Dokl Biochem Biophys, 2023, 513 (1): 350-354.

[24] Shafeghat M, Kazemian S, Aminorroaya A, et al. Toll-like receptor 7 regulates cardiovascular diseases [J]. Int Immunopharmacol, 2022, 113 (Pt A): 109390.

[25] Ain QU, Sarfraz M, Prasesti GK, et al. Confounders in identification and analysis of inflammatory biomarkers in cardiovascular diseases [J]. Biomolecules, 2021, 11 (10): 1464.

[26] Liu X, Bao Y, Lin Z, et al. Platelets inhibit development of atherosclerosis in atherosclerotic mice [J]. Cell Cycle, 2022, 21 (11): 1222-1232.

[27] Nguyen HT, Nguyen HT, Islam MZ, et al. Antagonistic effects of gingko biloba and sophora japonica on cerebral vasoconstriction in response to histamine, 5-hydroxytryptamine, U46619 and bradykinin [J]. Am J Chin Med, 2016, 44 (8): 1607-1625.

[28] Zhao L, Liu ZM, Piao ZZ. Clinical and experimental study on cerebral thrombosis treated with antithrombotic xinmaining [J]. Chinese Journal of Modern Developments

in Traditional Medicine, 1991, 11 (6): 327-330+323.

[29] Ridker PM, Tuttle KR, Perkovic V, et al. Inflammation drives residual risk in chronic kidney disease: A CANTOS substudy [J]. Eur Heart J, 2022, 43 (46): 4832-4844.

[30] Jia Q, Cao H, Shen D, et al. Quercetin protects against atherosclerosis by regulating the expression of PCSK9, CD36, PPARgamma, LXRalpha and ABCA1 [J]. Int J Mol Med, 2019, 44 (3): 893-902.

[31] Luo D, Yu B, Sun S, et al. Effects of adjuvant berberine therapy on acute ischemic stroke: A meta-analysis [J]. Phytother Res, 2023, 37 (9): 3820-3838.

[32] Mou Q, He J, Yin R, et al. Response surface optimized Infrared-Assisted extraction and UHPLC determination of flavonoid types from Flos Sophorae [J]. Molecules, 2017, 22 (6): 1000.

[33] Xie Z, Sun Y, Lam S, et al. Extraction and isolation of flavonoid glycosides from Flos Sophorae Immaturus using ultrasonic-assisted extraction followed by high-speed countercurrent chromatography [J]. J Sep Sci, 2014, 37 (8): 957-965.

[34] Liu JL, Li LY, He GH. Optimization of microwave-assisted extraction conditions for five major bioactive compounds from Flos Sophorae Immaturus (cultivars of *Sophora japonica* L.) using response surface methodology [J]. Molecules, 2016, 21 (3): 296.